NANO LETTERS

2007
Vol. 7, No. 12
3808−3812

A Golden Bullet? Selective Targeting of *Toxoplasma gondii* Tachyzoites Using Antibody-Functionalized Gold Nanorods

Dakrong Pissuwan,[†] Stella M. Valenzuela,[‡] Catherine M. Miller,[§] and Michael B. Cortie*[,†]

Institute for Nanoscale Technology, Department of Medical and Molecular Biosciences, Institute for the Biotechnology of Infectious Diseases, University of Technology Sydney, Australia

Received September 16, 2007; Revised Manuscript Received November 9, 2007

ABSTRACT

Conjugates of gold nanoparticles and antibodies have useful functionalities. Here, we show how they can be used to selectively target and destroy parasitic protozoans. Gold nanorods were conjugated with an anti-*Toxoplasma gondii* antibody and used to target the extracellular tachyzoite which is an infectious form of an obligate parasite *Toxoplasma gondii*. Subsequent laser irradiation was used to kill the targeted protozoans. This concept provides a new paradigm for the treatment of parasitic protozoans.

There has been some interest recently in the use of gold nanoparticles of various shapes for experimental photothermal therapies.[1−3] In particular, the enhanced absorption and scattering of gold nanoshells and nanosphere aggregates have been investigated for thermal therapy and biological imaging.[4−8] Gold nanorods are also promising candidates for exploitation in thermal therapy because they can be readily synthesized to selectively absorb in the near-infrared, a region in which the body is relatively transparent. Gold nanorods provide a higher efficiency of light absorption at their longitudinal plasmon resonance than any other known nanoparticles, including nanoshells.[9] They have recently been used to target tumor cells[3,10,11] and macrophages by this means.[12,13] The optical extinction peaks of nanorods generally display higher efficiencies (at longitudinal resonance) than those of nanospheres or nanoshells due to the longitudinal direction of the nanorod being significantly longer than the mean free path of electrons in that material.[14] These factors suggest that gold nanorods would be a suitable, if not actually superior, candidate for a variety of spectrally selective optical applications.[15,16] In the present work, we examine whether they can be used in a photothermal medical context to destroy a new type of target: parasitic protozoans. In particular, we have selected the organism *Toxoplasma gondii* as a model on which to test our ideas. Our work is performed in vitro. Ultimately, however, the objective is to develop an in vivo technique to kill infectious protozoans using nanorod photothermal therapy.

Toxoplasma gondii (*T. gondii*) is an intracellular protozoan parasite that has a worldwide distribution in humans and animals. Human infection rates vary from 10−90% in different countries depending on factors such as prevalence in animals and dietary habits.[17] Although infection with *T. gondii* results in a benign chronic infection in immunocompetent individuals, serious disease (toxoplasmosis) can occur if infection is acquired through congenitial infection or by immunosuppressed individuals such as AIDS patients or organ transplant recipients.[18.] There are three infectious forms in the life cycle of *T. gondii*: tachyzoites, bradyzoites, and sporozoites. Acute infection is characterized by the proliferation of the rapidly dividing tachyzoite stage. Tachyzoites are able to actively invade all nucleated cell types of warm-blooded vertebrate hosts and form a parasitiphorous vacuole in the cytoplasm. There they replicate until the host cell lyses. After death of the host cell, the newly liberated tachyzoites spread via the bloodstream, invade neighboring cells, and start replicating again.[19−21]

Gold nanorods were prepared by a seed-mediated growth method.[13,22] Briefly, a seed solution of gold nanoparticles was prepared by reaction of 0.10 mL of 0.02 M KBH_4 and 10 mL of an aqueous solution containing 0.5 mM $HAuCl_4$ and 0.2 M cetyltrimethylammonium bromide (CTAB). After stirring vigorously for 30 min, 12 μL of the seed solution was added to a growth solution at room temperature. The growth solution was prepared by adding 0.10 mL of 0.10 M L-ascorbic acid into 10 mL of aqueous solution containing

* Corresponding author. E-mail: michael.cortie@uts.edu.au.
[†] Institute for Nanoscale Technology.
[‡] Department of Medical and Molecular Biosciences.
[§] Institute for the Biotechnology of Infectious Diseases.

10.1021/nl072377+ CCC: $37.00
Published on Web 11/23/2007

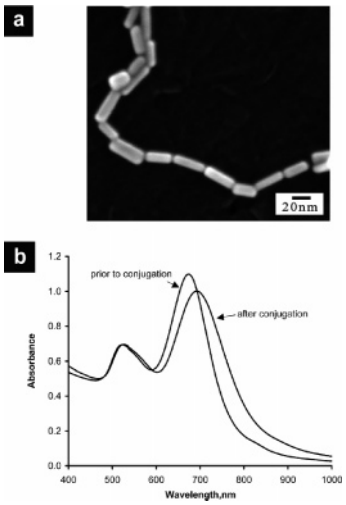

Figure 1. Characterization of gold nanorods. **(**a) Unconjugated gold nanorods imaged in a scanning electron microscope. (b) The absorbance spectra of conjugated and unconjugated gold nanorods. The absorption peak of the transverse plasmon resonance is around 520 nm and is not significantly changed by conjugation. However, the longitudinal plasmon resonance is red-shifted from 675 to 692 nm by conjugation.

0.1 mL of 10 mM $AgNO_3$, 0.2 M CTAB, and 0.5 mM $HAuCl_4$. The formation of rods proceeded over a period of several minutes and was associated with a change in color from the purple-red characteristic of gold nanospheres to a deep blue. Any large spherical particles that formed were removed by gentle centrifugation (3700 rpm for 5 min). The rest of the colloid was doubly centrifuged and washed (8000 rpm for 15 min with Milli Q water) to remove CTAB not bound to the nanorods, which would be cytotoxic.[23] Care was taken not to disturb the pellet during the CTAB removal process. The pH of sol was then adjusted to 7.5 by dropwise addition of 0.5 M KOH, at which point the gold nanorods were safe for use with cells and ready for conjugation with antibody.

After washing, a small drop of gold nanorod solution was dried on a clean carbon stub and stored in a desiccator before imaging with a scanning electron microscope. The rods were an average of 39.5 $\pm$ 0.5 nm in length and 20.0 $\pm$ 0.1 nm in width (Figure 1a). A transverse plasmon resonance at 522 nm and a longitudinal plasmon resonance at 674 nm were evident in the optical extinction spectra (Figure 1b). Anti-*T. gondii* antibody (anti-*Toxoplasma gondii* 30 kDa antibody, Argene Biosoft) raised against the major antigen on the surface of *T. gondii* tachyzoite (RH strain) was then conjugated to the gold nanorods to ensure selective attachment to free tachyzoites. The amount of antibody used was sufficient to stabilize and prevent aggregation of gold nanoparticles. The mechanism of conjugation is believed to be electrostatic in nature, with some negatively charged part of the antibody molecule being attracted to the positively charged CTAB sheath of the nanorod. We do not believe that the CTAB is displaced in this process. The variation in pH is not believed to have any effect on the surface charge of the gold nanorod itself,[24] and the requirement to fix the pH at 7.5 may follow from the effect that pH is likely to have on the conformation of the antibody molecule. However, the detailed mechanism by which this conjugation occurs is not yet clear, and the optimum conjugation conditions must be determined empirically. After 10 min incubation, the unbound antibody was removed by centrifugation at 8000 rpm for 15 min, followed by washing in phosphate buffer saline (PBS; no Ca^{2+} or Mg^{2+}) plus 1% bovine serum albumin (BSA). The working solution of gold−antibody conjugate was adjusted by dilution to an absorbance of 1.0 at the wavelength of peak extinction of the conjugated nanorods. After conjugation, the longitudinal plasmon peak of the nanorods moved to 692 nm and broadened (Figure 1b). This red shift may have been caused by an increase in local refractive index due to the antibody. The extinction peak is well positioned within the so-called "tissue window", a region, extending from about 650 to 850 nm, in which body tissue is comparatively more transparent to light.[25,26] (Although blood pigments in deep tissue can strongly absorb near-infrared light, the resulting heat is rapidly dissipated by the circulation.[27,28])

Tachyzoites were prepared by growing *Toxoplasma gondii* (RH strain) in African green monkey kidney (Vero) cells. Briefly, cells and tachyzoites were grown in RPMI 1640 medium (JRH Bioscience) containing 2% 1 M HEPES buffer, 10 mL/L penicillin-streptomycin (Sigma-Aldrich), and supplemented with 2% fetal bovine serum (JRH Bioscience). Cells and tachyzoites were maintained in a 5% CO_2 humidified incubator at 37 °C. Tachyzoites were harvested after spontaneous lysis of Vero cells (about 3−4 days after infection) by centrifugation at 1500 rpm for 5 min to remove host cell debris. The supernatant portion was centrifuged again at 3700 rpm for 5 min, and the resulting pellet resuspended in RPMI supplemented with 2% fetal bovine serum. Tachyzoites were counted using a Neubauer hemeocytometer and the concentration adjusted to $1-3 \times 10^7$ tachyzoites/mL. Vero cells and human leukemic monocyte lymphoma cells (U937 line) were cultured in RPMI 1640 medium containing 2% 1M HEPES buffer, 10 mL/L penicillin-streptomycin, and supplemented with 5 and 10% fetal bovine serum, respectively.

The nanorod-antibody conjugates were then attached to the tachyzoites by incubation in vitro for 30 min at 37 °C and 5% CO_2. After incubation, tachyzoites were washed twice with PBS + 1% BSA by centrifugation for 5 min at 3700 or 1500 rpm for nonspecific (cell U937) followed by further attachment of secondary antibody; goat anti-mouse labeled with fluorescein isothiocyanate (FITC) to confirm the presence of the gold conjugate (Figure 2).

Green fluorescent staining from FITC on the secondary antibody was observed at the surface of the tachyzoites, indicating that the gold nanorods were functionalized with anti-*T. gondii* antibody (Figure 3a) and had selectively attached to the surface of the tachyzoites. A positive control was obtained by exposing the tachyzoites to the anti-*T.gondii* antibody and then to the secondary goat anti-mouse FITC antibody. This showed a similar pattern of fluorescence (Figure 3b, the difference in intensity is not significant and simply reflects a different camera condition). Negative

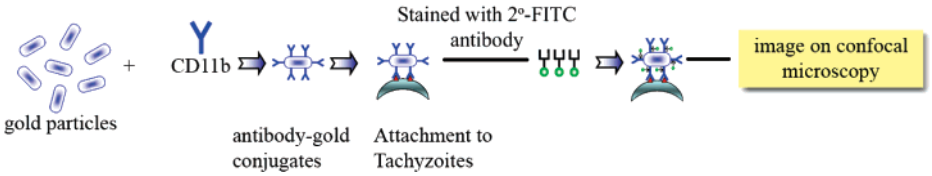

Figure 2. Schematic illustration of the method by which gold nanorods were attached to target protozoan and characterized.

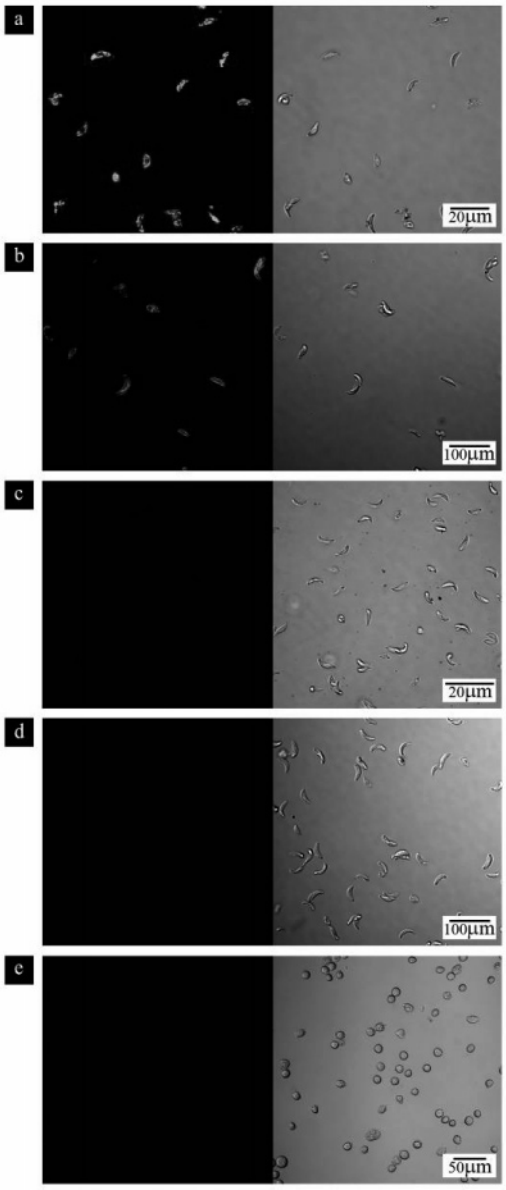

Figure 3. Fluorescent (left) and transmitted light (right) images of *T. gondii* tachyzoites and U937 cells (a) *T. gondii* tachyzoites incubated with anti-*T. gondii*−gold conjugates followed by exposure to goat anti-mouse IgG secondary−FITC antibody (2abFITC). **(**b) *T. gondii* tachyzoites incubated with anti-*T. gondii* antibody (anti-*T. gondii*), followed by exposure to 2abFITC. (c) *T. gondii* tachyzoites incubated with BSA−gold conjugates following with 2abFITC. (d) *T. gondii* tachyzoites incubated with 2abFITC only. (e) U937 cells incubated with anti-*T. gondii*−gold conjugates and followed by exposure to 2abFITC.

control staining was done similarly but with bovine serum albumin (BSA)/gold nanorod conjugates. In these cells, the fluorescent image was dark due to a lack of fluorescent staining (Figure 3c) indicating that the functionalized gold nanorods with nonspecific protein or antibody could not bind to the targeted cells (tachyzoites). Incubation of tachyzoites with secondary FITC antibodies alone also did not show any fluorescent staining (Figure 3d). An additional control experiment to demonstrate selective targeting was undertaken by incubating anti-*T. gondii*−gold nanorod conjugates with a nonspecific target, the human monocytic cell line, U937. As expected, no fluorescent staining was observed on the surface of these U937 cells (Figure 3e).

Having successfully achieved the selective attachment of gold nanorods to the tachyzoites, we then examined the extent to which they could be destroyed by laser irradiation. Tachyzoites were incubated with anti-*T. gondii*−gold nanorod conjugates, then a 3 μL droplet of tachyzoites with anti-*T. gondii*−gold nanorod conjugates was irradiated with a laser light from a 100 mW continuous wave diode laser (650 nm, Oatley Electronics) at power densities ranging between 0 and ~51 W/cm^2 for 4 min. Longer times would have produced a greater fluence (J/cm^2) and a higher final temperature, a process determined by heat transfer considerations.[13] The power density was controlled by varying the laser spot size. The controls included using unconjugated gold nanorods with tachyzoites to determine the proportion of nonspecific killing and U937 cells with conjugated rods to determine the proportion of nontargeted cells that would be destroyed.

The number of dead tachyzoites was determined by examination under the fluorescent mode of a confocal microscope after staining with SYTOX nucleic acid green dye. Fifteen fields from three triplicate runs of each treatment were counted under a magnification of at least 500× for cell viability. No less than 100 cells in each field were counted for every experimental condition. The natural endogenous cytochromes of cells normally have such a low absorption of light at this wavelength that application of laser irradiation alone does not destroy them.[29] In contrast, tachyzoites that had antibody-nanorod conjugates specifically bound to them were found to be strongly effected by laser irradiation. The percentage of cell death (Figure 4) rose from 18.8 ± 7.6% at the lowest power density (~0.7 W/m^2) to 82.9 ± 4.2% at the highest power density (~51 W/m^2). In contrast, a control sample of untreated gold−antibody conjugate tachyzoites that had been irradiated contained an average of 14.7 ± 3.7% dead tachyzoites, irrespective of the laser power applied (Figure 4). This was comparable to the sample of control tachyzoites that had not been irradiated at all (which contained 15.0 ± 3.9% dead tachyzoites). These results are consistent with a mechanism in which the plasmon resonance of the gold nanorods causes localized heating in the vicinity

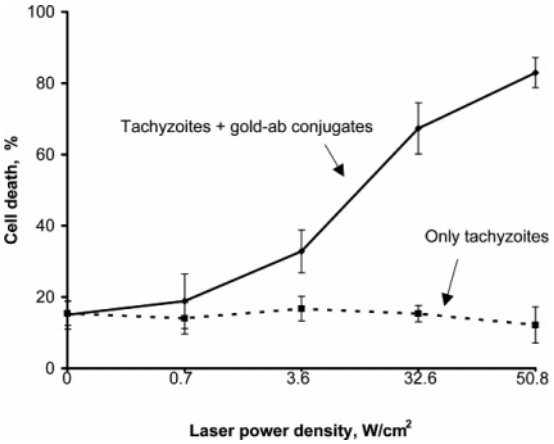

Figure 4. The cell death rates of *T. gondii* tachyzoites that had been labeled with gold nanorod−antibody conjugates compared to that of nonlabeled *T. gondii* tachyzoites (The laser diode used had $\lambda = 650$ nm and a power of 100 mW).

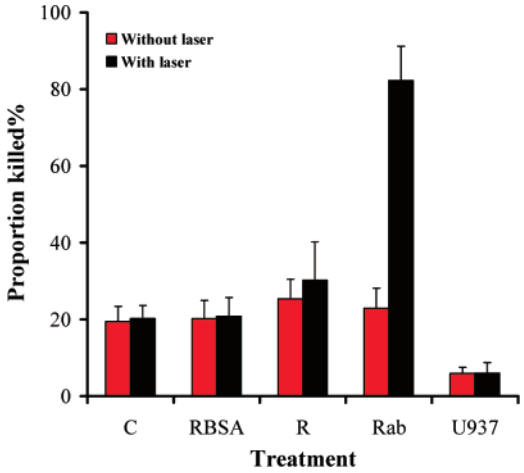

Figure 5. Effect of laser irradiation on *T. gondii* tachyzoites and U937 cells under various conditions. The power density of the laser was ~51 W/cm^2. (Error bars correspond to standard deviation from the mean.) Key: C = *T. gondii* tachyzoites only, R = *T. gondii* tachyzoites incubated with unconjugated gold, RBSA = *T. gondii* tachyzoites incubated with gold−BSA conjugates, Rab = *T. gondii* tachyzoites incubated with gold−antibody conjugates, and U937 = U937 cells incubated with gold−antibody conjugates. (Antibody means anti-*T. gondii* surface antigen.)

of the membrane of the targeted cell, which in turn induces hyperthermia leading to destruction of the cell.[10,11,13] A separate study of the effect of temperature on the viability of *T. gondii* tachyzoites (data in Supporting Information) shows that they are killed at a temperature of 60 °C or higher. This implies that the temperature generated from the interaction between the laser light and the gold nanorods would have been at least 60 °C. The total numbers of gold nanorods per tachyzoites were not determined in these experiments. Rather, the concentration of gold nanorod-antibody conjugates was adjusted to an optical density value of 1.0 at the wavelength of peak extinction (675 nm). This had been found to be a sufficient concentration to destroy tachyzoites at the highest power density (~51 W/m^2).

The numbers of dead tachyzoites in the control sample and that in which anti-*T. gondii*−gold nanorod conjugates had been attached to the cells was 15.0 ± 3.9 and 15.5 ± 3.4% respectively. These results support the contention that it was neither the gold rods alone nor the CTAB on them that caused cell death.

A further series of control experiments were run at a laser power density of ~51 W/cm^2. Nonspecific binding of gold nanorods was investigated by using unconjugated gold nanorods incubated with the tachyzoites for 30 min. In this case, the percentage of cell death after irradiation was 30.2 ± 10.0%, which was slightly higher than the 25.4 ± 5.1% death rate in tachyzoites that had not been exposed to the laser in this experiment (Figure 5). It should be noted that the initial viability of the tachyzoites for this particular set of experiments was ~80% (Figure 5), compared to ~85% (Figure 4) for the tachyzoites exposed to the various laser power densities. We found that 15 ± 5% of extracellular tachyzoites recovered from a lysed monolayer were nonviable in every experiment performed. This level of nonviable tachyzoites is consistent with other reports of in vitro culture of *T. gondii* in Vero cells. Even when culture conditions are very closely monitored, 100% viability of tachyzoites is never achieved. The infection ratio between host cells and tachyzoites also impacts on tachyzoite viability[30] This is partly due to the fact that it is difficult to synchronize exact timing between lysis of infected host cells by tachyzoites and the subsequent use of the released tachyzoites for infection of a newly established host cell monolayer.[31] It appears that not all tachyzoites released are able to invade new cells in the monolayer and they do not survive long outside a host cell. This therefore also impacts upon the cell viability of the tachyzoites. The slight variation in viability can also be accounted for by use of different generations of tachyzoites and differences in the harvest time.

Tachyzoites were also incubated with nanorods that had been conjugated with BSA, followed by exposure to laser or no laser irradiation. The percentage of dead tachyzoites from these two groups was found to be very similar at around 20 ± 5%. These results suggest that naked gold nanorods have a tendency to adhere to the tachyzoites, but BSA conjugated nanorods do not. Nonspecific binding and uptake of unconjugated gold nanorods by other cells has also been reported recently and is evidently a general property of naked gold nanoparticles,[12,32,33] which in the present instance is undesirable. However, we have shown in this paper and another[12] that coating gold nanoparticles with nonspecific protein, such as BSA, decreased their nonspecific uptake by host cells. Nevertheless, any future in vivo experiment will additionally have to consider what the effect would be of antibody-conjugated gold nanorods that for some reason have not bound to a target cell prior to laser irradiation. Such particles will introduce a measure of untargeted heat generation and would have to be minimized.

A further indication of the specificity of the photothermal effect was obtained by incubating U937 cells with anti-*T. gondii*−gold nanorod conjugates. In this case, the number of dead U937 cells was not different from nonirradiated cells (5.9 ± 1.57 and 6.0 ± 2.7% for irradiated and nonirradiated cells, respectively) even at the highest power density. In contrast, tachyzoites incubated with anti-*T. gondii*−gold

nanorod conjugates had a death rate of 82.2 ± 9.0% after laser irradiation at the same power (Figure 5). This is also encouraging as use of these conjugates in vivo would be required to have minimal binding to host cells.

We have shown how the idea of using plasmonic heating in nanoparticles to target tumor cells can be extended to kill the extracellular tachyzoites of a pathogenic parasite. Of course, the tachyzoite stage of the *T. gondii* model studied here can already be treated by drugs such as sulfonamide and pyrimethamine. However, the side effects and level of therapy from these drugs need to be considered,[34,35] and in any case the availability of a completely new treatment paradigm is always potentially useful. Furthermore, the new paradigm is general in nature and can be readily extended to address many other species of pathogenic organism.

Acknowledgment. This work was supported by the University of Technology Sydney. We thank Dr. Xiaoda Xu for synthesis of the gold nanorods and Dr. Michael Johnson for technical support.

Supporting Information Available: Graph and text describing effect of temperature on viability of *Toxoplasma gondii* tachyzoites. This material is available free of charge via the Internet at http://pubs.acs.org.

References

(1) Hirsch, L. R.; Stafford, R. J.; Bankson, J. A.; Sershen, S. R.; Rivera, B.; Price, R. E.; Hazle, J. D.; Halas, N. J.; West, J. L. *Proc. Natl. Acad. Sci. U.S.A.* **2003**, *100* (23), 13549−13554.
(2) Pissuwan, D.; Valenzuela, S.; Cortie, M. B. *Trends Biotechnol.* **2006**, *24* (2), 62−67.
(3) El-Sayed, I. H.; Huang, X.; El-Sayed, M. A. *Cancer Lett.* **2006**, *239* (1), 129−135.
(4) Hirsch, L. R.; Jackson, J. B.; Lee, A.; Halas, N. J.; West, J. L. *Anal. Chem.* **2003**, *75*, 2377−2381.
(5) O'Neal, D. P.; Hirsch, L. R.; Halas, N. J.; Payne, J. D.; West, J. L. *Cancer Lett.* **2004**, *209* (2), 171−176.
(6) Loo, C.; Lin, A.; Hirsch, L.; Lee, M. H.; Barton, J.; Halas, N.; West, J.; Drezek, R. *Technol. Cancer Res. Treat.* **2004**, *3* (1), 33−40.
(7) Zharov, V. P.; Galitovskaya, E. N.; Johnson, C.; Kelly, T. *Lasers Surg. Med.* **2005**, *37*, 219−226.
(8) Zhang, J. Z.; Schwartzberg, A. M.; Norman, T., Jr.; Grant, C. D.; Liu, J.; Bridges, F.; van Buuren, T. *Nano Lett.* **2005**, *5*, 809−810.
(9) Jain, P. K.; Lee, K. S.; El-Sayed, I. H.; El-Sayed, M. A. *J. Phys. Chem. B* **2006**, *110*, 7238−7248.
(10) Huang, X.; El-Sayed, I. H.; Qian, W.; El-Sayed, M. A. *J. Am. Chem. Soc.* **2006**, *128* (6), 2115−2120.
(11) Huff, T. B.; Tong, L.; Zhao, Y.; Hansen, M. N.; Cheng, J. X.; Wei, A. *Nanomedicine* **2007**, *2* (1), 125−132.
(12) Pissuwan, D.; Cortie, C. H.; Valenzuela, S.; Cortie, M. B. *Gold Bull.* **2007**, *40* (2), 121−129.
(13) Pissuwan, D.; Valenzuela, S. M.; Killingsworth, M. C.; Xu, X.; Cortie, M. B. *J. Nanopart. Res.* **2007**, *9* (6), 1109−1124.
(14) Kooij, E. S.; Poelsema, B. *Phys. Chem. Chem. Phys.* **2006**, *8*, 3349−3357.
(15) Sonnichsen, C.; Franzl, T.; Wilk, T.; Plessen, G. v.; Feldmann, J. *Phys. Rev. Lett.* **2002**, *88* (7), 077402−1−4.
(16) Xu, X.; Gibbons, T.; Cortie, M. B. *Gold Bull.* **2006**, *39* (4), 156−165.
(17) Stoicov, C.; Whary, M.; Rogers, A. B.; Lee, F. S.; Klucevsek, K.; Li, H. C.; Cai, X.; Saffari, R.; Ge, Z. M.; Khan, I. A.; Combe, C.; Luster, A.; Fox, J. G.; Houghton, J. M. *J. Immunol.* **2004**, *173* (5), 3329−3336.
(18) Alibertie, J. *Nat. Rev. Immunol.* **2005**, *5*, 162−170.
(19) Tenter, A.; Heckeroth, A. R.; Weiss, L. M. *Int. J. Parasitol.* **2000**, *30*, 1217−1258.
(20) Montoya, J. G.; Liesenfeld, O. *Lancet* **2004**, *363*, 1965−1976.
(21) Ambroise-Thomas, P.; Petersen, E. *Congenital Toxoplasmosis*; Springer: New York, 2000.
(22) Nikoobakht, B.; El-Sayed, M. A. *Chem. Mater.* **2003**, *15*, 1957−1962.
(23) Connor, E. E.; Mwamuka, J.; Gole, A.; Murphy, C. J.; Wyatt, M. D. *Small* **2005**, *1* (3), 325−327.
(24) Orendorff, C. J.; Hankins, P. L.; Murphy, C. J. *Langmuir* **2005**, *21*, 2022−2026.
(25) Weissleder, R. *Nat. Biotechnol.* **2001**, *19*, 316−317.
(26) Simpson, C. R.; Kohl, M.; Essenpreis, M.; Copey, M. *Phys. Med. Biol.* **1998**, *43*, 2465−2478.
(27) Pogue, B. W.; Lilge, L.; Patterson, M.; Wilson, B.; Hasan, T. *Appl. Opt.* **1997**, *36* (28), 7257−7269.
(28) Bozkurt, A.; Onaral, B. *Biomed. Eng. Online* **2004**, *3* (1), 9.
(29) Vladimirov, Y. A.; Osipov, A. N.; Klebanov, G. I. *Biochemistry* **2004**, *69* (1), 81−90.
(30) Evans, R.; Chatterton, J. M. W.; Ashburn, D.; Joss, A. W. L.; Ho-Yen, D. O. *Eur. J. Clin. Microbiol. Infect. Dis.* **1999**, *18*, 879−884.
(31) Woodmansee, D. B. *J. Parasitol.* **2003**, *89* (5), 895−898.
(32) Huff, T. B.; Hansen, M. N.; Zhao, Y.; Cheng, J.-X.; Wei, A. *Langmuir* **2007**, *23*, 1596−1599.
(33) Chithrani, B. D.; Ghazani, A. A.; Chan, W. C. W. *Nano Lett.* **2006**, *6* (4), 662−668.
(34) Black, M. W.; Boothroyd, J. C. *Microbiol. Mol. Biol. Rev.* **2000**, *64* (3), 607−623.
(35) Tenant-Flowers, M.; Boyle, M. J.; Carey, D. *AIDS* **1991**, *5* (3), 311−316.

NL072377+